Rayleigh and Compton Scattering Cross-sections for 19.648 keV Photons

Prem Singh

Dept. of Physics, S.D. College Ambala Cantt.-133001, Haryana, India
pspundir1@gmail.com

Abstract: Rayleigh and Compton scattering differential cross-sections for the 19.648 keV photons in a few elements with $6 \leq Z \leq 50$ have been measured. These measurements were performed under vacuum ($\sim 10^{-2}$ Torr) at 141° scattering angle in secondary reflection mode geometrical arrangement using $_{42}MoK_{\beta}$ x-ray photons excited by ^{241}Am radioisotope as the primary photon source and an HPGe/Si(Li) detector. Measured cross-sections for the Rayleigh scattering are compared with the modified form-factors (MFs), the MFs corrected for the anomalous scattering factors (ASFs), i.e., MFASFs and the S-matrix calculations. The measured Compton scattering cross-sections are compared with the theoretical Klein-Nishina cross-sections corrected for the non-relativistic Hartree-Fock incoherent scattering function S(x, Z). [Prem Singh. Rayleigh and Compton Scattering Cross-sections for 19.648 keV Photons. [Prem Singh**. Rayleigh and Compton Scattering Cross-sections for 19.648 keV Photons**. Nature and Science 2011;9(10):70-77]. (ISSN: 1545-0740). http://www.sciencepub.net. #9

Keywords: Rayleigh and Compton Scattering; Radioisotope; Photons; cross-sections

1. Introduction

Scattering is an important mode of photon-atom interaction and the scattering contribution from electrons dominates in the x-ray energy region. In the elastic scattering process, the energy of the scattered photons remains same as that of the incident photon and only the momentum is changed. Elastic scattering of photons from bound electrons is known as Rayleigh scattering [Roy *et al*, 1999]. In the inelastic scattering process, energy of the scattered photon is less than that of the incident photons. Inelastic scattering leads to either ionization or excitation of the atom. Inelastic scattering, which leads to ionization of the atom is known as Compton scattering and that leads to excitation of the atom is known as Raman scattering. Rayleigh scattering cross-sections exhibit a considerable variation with the atomic number (Z) whereas the Compton scattering cross-sections vary feebly. Rayleigh scattering measurements give information about the material from its atomic number (Z) [Karydas *et al*, 1993] and the Compton scattering measurements give information about the physical parameters, such as electron density, target mass and the mass thickness [Spran *et al*, 1998].

The major theoretical approaches developed for Rayleigh scattering are based on the (i) form-factor (FF) formalism [Hubbell *et al*, 1979, Schaupp *et al*, *1983*] and (ii) second order S-matrix calculations [Kissel *et al*, 1995, Kissel, 2000]. The form-factor calculations are not valid at photon energies near to the electron binding energies of the elements and dispersion corrections, popularly known as anomalous scattering factors (ASFs), [Cromer *et al*, 1981, Kissel *et al*, 1990] become important in such cases. Theoretical S-matrix values are the most sophisticated calculations, which are available both for the Rayleigh [Kissel, 1997] and the Compton scattering [Bergstrom *et al*, 1993]. Compton scattering differential cross-sections are conveniently expressed in terms of the cross-section for photon scattering by an electron (Klein-Nishina cross-section) and the incoherent scattering function (ISF) [Hubbell *et al*1975] representing the probability that the atomic electron, having received momentum x $(=2(h\nu/c)\sin(\theta/2))$ will absorb an amount of energy resulting in excited or ionized atomic state.

Most of the scattering experiments were performed in the direct mode geometrical arrangement [Singh *et al*, 2004, Shahi *et al*, 1998, Casnati *et al*, 1990, Elyaseery *et al*, 1998] either using the radioisotopes or x-ray tube. Some of the measurements [Singh *et al*, 2004, Singh *et al*, 2006, Kumar *et al*, 2002] are available in the low energy region. In the lower energy region, an accurate knowledge of scattering cross-sections is particularly important near the electron binding energies. Kumar *et al* [Kumar *et al*, 2007] have measured the elastic, Compton and K-shell radiative resonant Raman scattering cross-sections in $_{83}Bi$ for the 88.034 keV γ-rays.

In the present work, a comparison of the experimentally measured Rayleigh and Compton scattering cross-sections to the theoretical predictions is presented. This comparison is done to provide a check for the theoretical calculations and to assess the need for future advances in both the experiment and theory. During the present measurements, special care was given to the factors that may cause systematic influence on the results.

2. Experimental Procedure

The scattering measurements have been performed using the secondary mode geometrical arrangement shown in figure 1. These measurements were performed using the 19.648 keV ($_{42}$Mo K_β) photons through an angle of 141°. The photon source consisted of the annular foil molybdenum excited by the 59.54 keV γ-rays from an annular radioactive source of ^{241}Am (300 mCi). The scattered photons were detected using planar HPGe and Si(Li) detectors (FWHM = 180 eV at 5.89 keV). Spectroscopically pure, self-supporting targets with thickness ranging 8-650 mg/cm^2 were used. Three spectra were taken for each target using a PC-based multichannel analyzer (Canberra, Model S-100) with acquisition time ranging 25-60 hours. For each target, the spectra were repeatedly taken from different portions of the target at different occasions. Typical spectra from the Si and Ti targets are shown in figures 2(a) and 2(b), respectively.

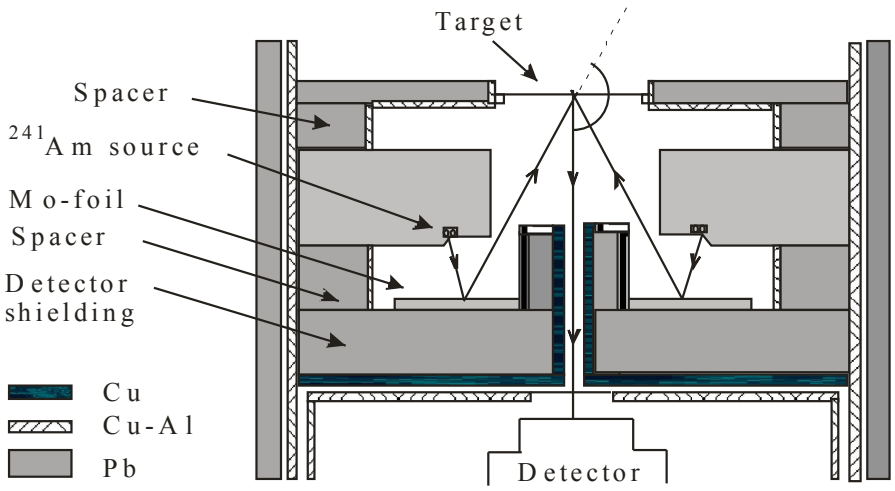

Figure 1. Geometrical arrangement used in the present measurements.

2.1 Evaluation Procedure

Measured differential cross-sections for the Rayleigh and Compton scattering of the 19.648 keV photons were evaluated using the relation

$$\left(\frac{d\sigma}{d\Omega}\right)_s = \frac{N_s}{4\pi (I_o G)_\beta \varepsilon_s m \beta} \qquad (1)$$

where N_s is the number of counts per second under the scatter 19.648 keV peak, $(I_oG)_\beta$ is the intensity of K_β x-ray photons from the Mo-foil falling on portion of the target visible to the detector, ε_s is efficiency of the detector at energy of the Rayleigh-scatter peak, m is the mass per unit area (gm/cm^2) of the element under investigation in the target and β is the absorption correction factor that accounts for absorption of the incident and scattered photons in the target. The values of β for the scattered photons have been evaluated using the mass-attenuation coefficients taken from Ref. [Hubbell *et al*, 1995, Storm *et al*, 1970] and using the relation

$$\beta = \frac{1-\left[\exp(-1)\left[\left(\mu/\rho\right)_1 \sec\theta_1 + \left(\mu/\rho\right)_2 \sec\theta_2\right]m\right]}{\left[\left(\mu/\rho\right)_1 \sec\theta_1 + \left(\mu/\rho\right)_2 \sec\theta_2\right]m} \qquad (2)$$

where $\left(\mu/\rho\right)_1$ and $\left(\mu/\rho\right)_2$ are the mass-absorption coefficients (cm^2/gm) of the target element corresponding to the incident and scattered photon energies, respectively. θ_1 and θ_2 are the angles formed by the incident and the scattered or emitted radiation with the normal to the sample surface respectively, m is the thickness of the target in gm/cm^2. For the geometry used in the present measurements, θ_2 is taken to be 0° as the fluorescent x-rays are presumed to strike the detector perpendicular to its surface. For the evaluation of β for Rayleigh scattering, the total minus coherent part of the mass attenuation coefficient has been used for the incident part and the total mass attenuation coefficient for the scattered part. The

photoabsorption part of the mass attenuation coefficients was used in the evaluation of β for the Compton scattering to take care of the multiple scattering. Each spectrum was analyzed for photopeak area under the Rayleigh and Compton-scatter K_β x-ray peaks from the Mo-foil using an indigenously developed computer code PEAKFIT [Singh *et al*, 1995].

The product of intensity of the K_β x-rays from the Mo-foil and efficiency of the detector at the elastic-scatter x-ray energy, $(I_o G)_\alpha \varepsilon_{sc}$, was interpolated from set of the $(I_o G)_\alpha \varepsilon_{KX}$ values. These values were determined over the energy range 8.6-16 keV by measuring the K_α and K_β x-rays from Ge, Se, Br, Sr and Y elements excited by the Mo *K* x-rays and using the expression

$$(I_o G)_\alpha \varepsilon_{KX} = \frac{N_{KX}}{m\left[\sigma_{KX}^{\alpha}\beta_{KX}^{\alpha} + \sigma_{KX}^{\beta}\beta_{KX}^{\beta}\dfrac{(I_o G)_\beta}{(I_o G)_\alpha}\right]} \quad (3)$$

where N_{KX} is the counts/s under the K_α or K_β x-ray peak of the element in the spectrum. The superscripts α and β correspond to the incident Mo K_α and K_β x-rays, respectively. σ_{KX}^{i} (i = α, β) is the *K* x-ray fluorescence cross-section for the target element at the Mo K_α and K_β x-ray energies, respectively, and has been interpolated from the tables of Puri *et al* [Puri *et al*, 1995]. $\dfrac{(I_o G)_\beta}{(I_o G)_\alpha}$ is the ratio of intensities of the K_β and K_α x-rays emitted from the Mo-foil.

3. Results and Discussions

The present measured Rayleigh scattering cross-sections for the 19.648 keV photons are compared in Table 1 with those evaluated using the form-factor approaches, namely, modified form-factor (MF), modified form-factor corrected for anomalous scattering factors (MFASF) and the second order S-matrix calculations. The percentage deviations of the theoretical values from the measured Rayleigh scattering cross-sections are also given in Table 1. The MF, MFASF and S-matrix Rayleigh scattering cross-sections are taken from ref. [Kissel, 1997]. The ASFs, g' and g'', used in the calculations of the MFASF cross-sections, were evaluated using the relativistic Hartree-Fock-Slater potential with Latter tail and taken to be angle independent. The experimentally measured and theoretical Rayleigh scattering cross-sections for the 19.648 keV photon energies are better compared as a function of atomic number in figure 3. The MFASF values are generally higher than the MF ones for the elements their binding energies away from incident photon energy. The MFASF values are less than the MF ones for the elements having their binding energies in the vicinity of the incident photon energy. The available S-matrix cross-sections for the elements under investigation match with the MFASF ones for the C, Al, Si and S elements and are lower upto 5% for the other elements under investigation for the 19.648 keV incident photon energy. For the 19.648 keV incident photon energy, the MF cross-sections are found to be lower than the measured ones upto 15% for the elements with $6 \le Z \le 34$ and higher up to 39% for the elements with $45 \le Z \le 50$. The largest deviation in the MF value from the measured cross-section is in the element $_{45}$Rh, having its K-shell binding energy close to the incident photon energy.

The experimentally measured and theoretical Compton scattering cross-sections for the 19.648 keV photon energies are compared in Table 2. The Compton scattering cross-sections measured using targets of different thickness were found to be consistent, which infer that the present β evaluation procedure takes care of the multiple scattering effects. The measured Compton scattering cross-sections for the 19.648 keV photons differ upto 9% from the theoretical ones. The measured Rayleigh to Compton scattering differential cross-section ratio as a function of atomic number (Z) is shown in figure 4. The ratios of theoretical S-matrix Rayleigh scattering to the KN+ISF Compton scattering cross-section are also plotted for comparison. The measured and the theoretical ratio follow the similar trends.

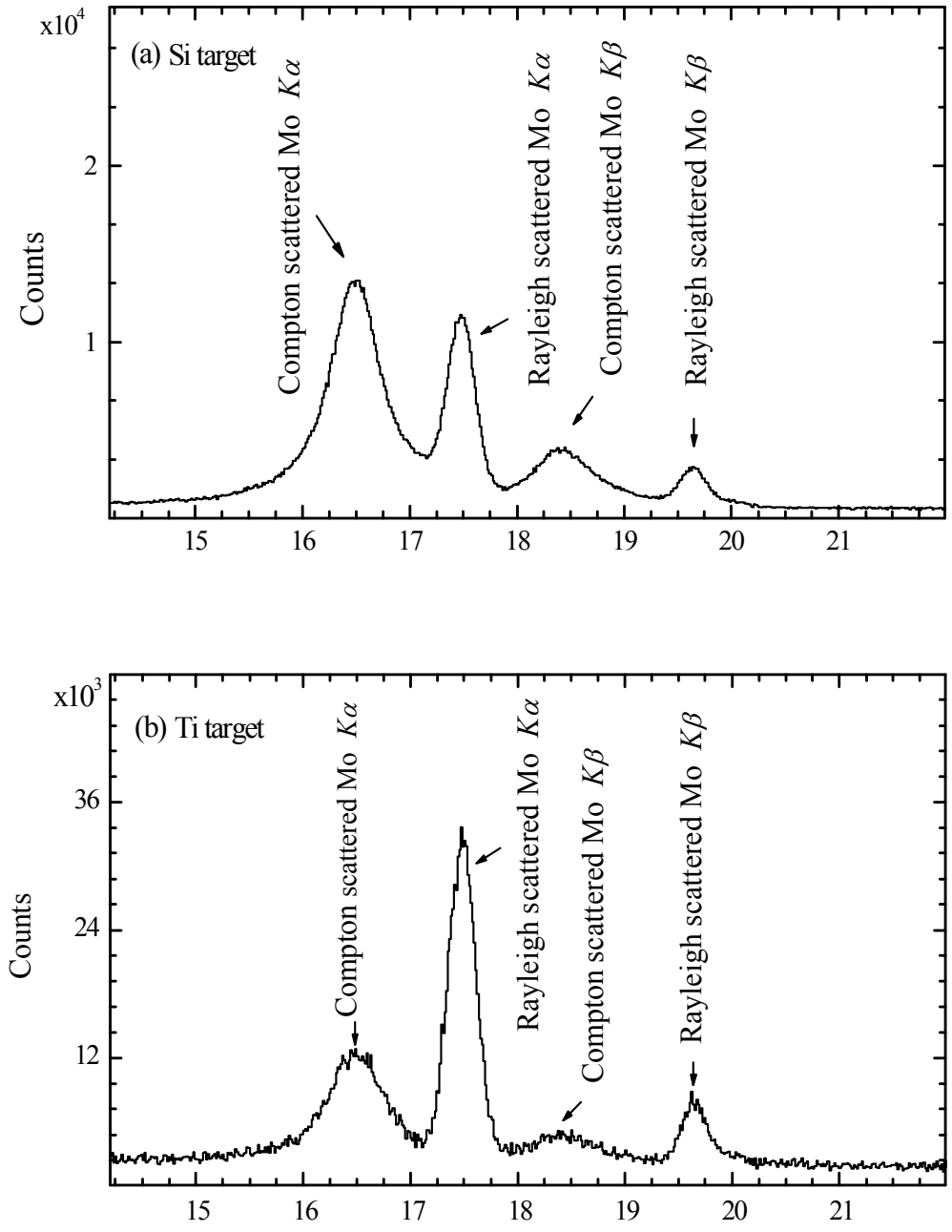

Figure 2. Typical spectra of the 19.648 keV photons scattered through an angle of 141° by (a) Si target and (b) Ti target.

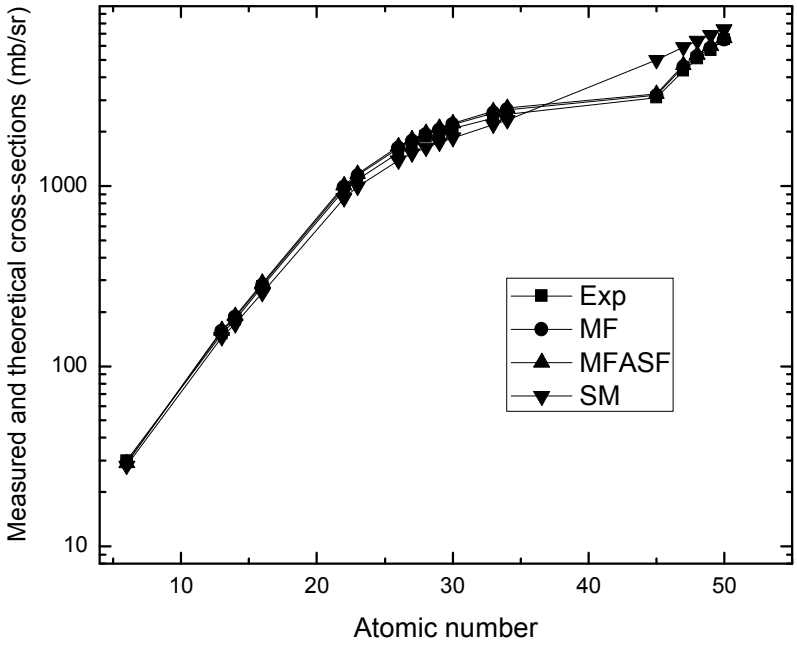

Figure 3. Measured and theoretical Rayleigh scattering cross-sections for different elements at 19.648 keV photon energy as a function of atomic number.

Table 1. Differential cross-sections for the Rayleigh scattering of the 19.648 keV photons through an angle of 141° [momentum transfer = 1.494 $Å^{-1}$].

Element (Z)	K-shell Binding Energy (keV)	Scattering cross-sections (mb/sr)				Percentage deviations from measured cross-sections		
		Experimental	Theoretical					
			S-matrix	MFASF	MF	S-matrix	MFASF	MF
C (6)	0.284	30	29	29	28	3	3	7
Al (13)	1.56	152	156	158	145	-3	-4	5
Si (14)	1.839	181	187	190	172	-3	-5	5
S (16)	2.472	278	283	289	255	-2	-4	9
Ti (22)	4.966	948	987	1009	860	-4	-6	10
V (23)	5.465	1087	1148	1172	995	-5	-7	9
Fe (26)	7.112	1531	1628	1662	1391	-6	-8	10
Co (27)	7.709	1673	1779	1816	1515	-6	-8	10

Ni (28)	8.332	1887	1925	1964	1634	-2	-4	15
Cu (29)	8.981	1966	2046	2102	1746	-4	-6	12
Zn (30)	9.659	2093	2194	2238	1859	-5	-6	12
As (33)	11.867	2387	2546	2602	2196	-6	-8	9
Se (34)	12.658	2506	2653	2711	2318	-6	-7	8
Rh (45)	23.22	3089	3188	3259	5024	-3	-5	-39
Ag (47)	25.514	4367	4595	4708	5907	-5	-7	-26
Cd (48)	26.711	5106	5218	5352	6385	-2	-5	-20
In (49)	27.94	5693	5842	5997	6883	-3	-5	-17
Sn (50)	29.2	6532	6471	6647	7396	1	-2	-12

Table 2. Differential cross-sections for the Compton scattering of 19.648 keV photons through an angle of 141° [momentum transfer = 1.494 $Å^{-1}$].

Element (Z)	Compton scattering cross-sections (mb/sr)		Percentage deviation from measured values
	Experimental	Theoretical	
H (1)	52	56	-7
C (6)	316	323	-2
Al (13)	596	648	-9
Si (14)	651	694	-6
S (16)	726	782	-7
Ti (22)	986	1024	-4
V (23)	997	1063	-6
Fe (26)	1108	1179	-6
Co (27)	1102	1217	-9
Ni (28)	1141	1254	-9
Cu (29)	1238	1291	-4
Zn (30)	1297	1327	-3

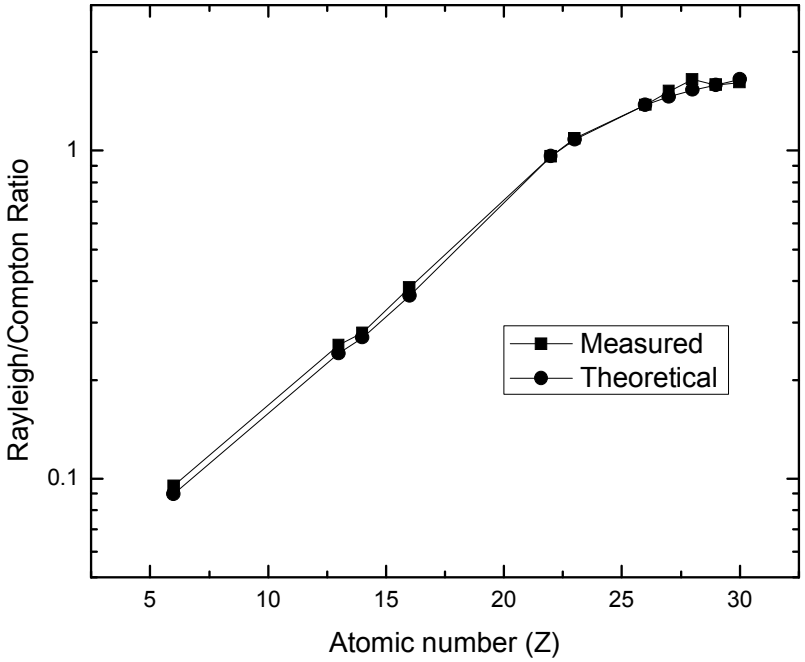

Figure 4. Rayleigh to Compton scattering differential cross-section ratio as a function of atomic number (Z).

4. Conclusions

In the present measurements, it is observed that the Rayleigh scattering cross-sections at low energies are significant enough even for the low-Z elements. In the Compton scattering measurements, the ISF and best-predicted results agree well at higher photon energies, but they are found to differ at energies below about 20 keV. At these energies it is known that ISF is not good due to the neglect of dynamic scattering term while the perturbative method used to obtain the best predictions at lower energies may not be completely adequate, both because the various perturbations become large and because they are not necessarily independent. For better insight, the relativistic second-order S-matrix calculations for the Compton scattering are desired for elements having electron binding energies close to the incident photon energy where the calculations based on the ISF approximation are found to deviate. Further measurements and theoretical calculations for different energies, angles and elements are needed to understand the general features of validity of theoretical calculations.

Acknowledgement: Author is highly thankful to Prof. (Dr.) Devinder Mehta, Dept. of Physics, Panjab University, Chandigarh for providing the EDXRF facility and useful suggestions during these measurements.

Correspondence to:
Dr. Prem Singh, Dept. of Physics,
S.D. College Ambala Cantt.,
Haryana, India-133001
Telephone: +91-171-2630283
Email: pspundir1@gmail.com

References

[1] Roy S.C., Kissel L. and Pratt R.H., Radiat. Phys. Chem. (1999): 56: 3.
[2] Karydas A.G. and Paradellis T., X-ray Spectrom. (1993): 22: 208.
[3] Spran Hans A.V. and Bekkers M.H.J., X-ray Spectrom. (1998): 27: 38.
[4] Hubbell J.H. and Øverbro I., J. Phys. Chem. Ref. Data (1979): 8: 69.
[5] Schaupp D., Schumacher M., Smend F., Rullhusen P. and Hubbell J.H., J. Phys. Chem. Ref. Data (1983): 12: 467.
[6] Kissel L., Zhou B., Roy S.C., Gupta S.K. Sen and Pratt R.H., Acta Cryst. A (1995): 51: 271.
[7] Kissel L., Radiat. Phys. and Chem. (2000): 59: 185.
[8] Cromer D.T., Libermann D.A., Acta Crystallogr. A (1981): 37: 267.
[9] Kissel L. and Pratt R.H., Acta Crystallogr. A (1990): 46: 170.
[10] Kissel L., Lawrence Livermore National Laboratory, USA (1997), Private

communication. Website: http://www-phys.llnl.gov/Research/scattering/.
[11] Bergstrom P.M., Suric T., Pisk K. and Pratt R.H., Phys. Rev. A (1993): 48: 1134.
[12] Hubbell J.H., Veigele W.J., Briggs E.A., Brown R.T., Cromer D.T. and Howerton R.J., Phys. Chem. Ref. Data (1975): 4: 471.
[13] Singh P., Mehta D., Singh N., Puri S., Shahi J.S., Nucl. Instrum. and Meth. B (2004): 225: 198 and references therein.
[14] Shahi J.S., Puri S., Mehta D., Garg M.L., Singh N. and Trehan P.N., Phy. Rev. A (1998): 57: 4327.
[15] Casnati E., Baraldi C. and Tartari A., Phy. Rev. A (1990): 42: 2627.
[16] Elyaseery I.S., Shukri A., Chong C.S., Tajuddin A.A. and Bradley D.A., Phy. Rev. A (1998): 57: 3469.
[17] Singh P., Puri S., Shahi J.S., Mehta D. and Singh N., Nucl. Instrum. and Meth. B (2004): 222: 1.
[18] Singh P., Kumar S., Goswamy J., Mehta D. and Singh N., Nucl. Instrum. and Meth. B (2006): 244: 295.
[19] Kumar A., Shahi J.S., Mehta D. and Singh N., Nucl. Instrum. and Meth. B (2002): 194: 105 and references therein.
[20] Kumar S., Sharma V., Mehta D. and Singh N., Nucl. Instrum. and Meth. B (2007): 264: 1.
[21] Hubbell J.H. and Seltzer S.M., National Institute of Standards and Technology Report No. NISTIR (1995): 5632 (unpublished).
[22] Storm E. and Israel H.I., Nucl. Data Tables A (1970): 7: 565.
[23] Singh J., Singh R., Mehta D., Singh N. and Trehan P.N., in proceedings of the DAE Symposium on Nuclear Physics, Nucl. Phys. B (1995): 37: 455.
[24] Puri S., Chand B., Mehta D., Garg M.L., Singh N. and Trehan P.N., At. Data Nucl. Data Tables (1995): 61: 289.

7/9/2011